doi:10.1007/s11589-011-0816-0

Anomaly of the ionospheric electron density close to earthquakes: Case studies of Pu'er and Wenchuan earthquakes*

Yufei He[1] Dongmei Yang[1,♣] Jiadong Qian[2] and Michel Parrot[3]

[1] *Institute of Geophysics, China Earthquake Administration, Beijing* 100081, *China*
[2] *Institute of Earthquake Science, China Earthquake Administration, Beijing* 100036, *China*
[3] *Laboratory of Physical and Chemical Environment, National Center for Scientific Research, Orleans* 45071, *France*

Abstract The electron density recorded onboard the DEMETER satellite was analyzed to search for possible anomalies before earthquakes both in space and time. To distinguish pre-earthquake anomalies from the other anomalies related to geomagnetic activity, data were filtered using the K_p index. The analysis is based on the comparison of data recorded closely to earthquakes in space and time and past data for the same area. In analyzing data around the time and location of the Pu'er and Wenchuan earthquakes, obvious anomalies in electron density were found close to the epicenters, and some remarkable disturbances were detected before the earthquakes occurred. The results were finally compared with those of previous works that used the same data but employed different analysis methods. Good agreement was found which suggests that these anomalies have a close relation to the earthquake preparation.

Key words: **Wenchuan earthquake; Pu'er earthquake; electron density; DEMETER satellite; anomaly**
CLC number: P315.72$^+$1 **Document code**: A

1 Introduction

In recent decades, ionospheric data have been used to investigate the earthquake precursors. Many papers and monographs have been published on seismo-ionospheric phenomena, and most of them were directly or indirectly concerned with ionospheric data (Larkina et a1., 1983; Chmyrev et a1., 1989; Parrot and Mogilevsky, l989; Molchanov, l993; Pulinets and Legenka, 2003). Widespread research on earthquake prediction has shown that earthquake precursors may exist not only in the lithosphere, but also in the atmosphere and the entire ionosphere from 100 km to 1 000 km through a coupling mechanism (Hayakawa, 1999; Hayakawa and Molchanov, 2002).

In recent years, as satellites for earthquake monitoring have been launched by many developed countries, an increasing number of seismo-ionospheric coupling phenomena have been reported. Since the launch of the first satellite dedicated to earthquake studies, there have been numerous reports on earthquake precursors (e.g., Parrot et al., 2006; Sarkar et al., 2007; Ouyang et al., 2008; Zhu et al., 2008; Nemec et al., 2008; He et al., 2009; Zhang et al., 2009; Rozhnoi et al., 2008, 2010; Akhoondzadeh et al., 2010). Lithosphere-atmosphere-ionosphere coupling has become a new field of theoretical research, and many hypotheses and much modelling have been published, however, some scientists did not agree on the interpretation of this coupling mechanism (e.g., Parrot and Mogilevsky, 1989; Parrot and Johnston, 1993; Gokhberg et al., 1983; Hayakawa, 1999; Pulinets and Boyarchuk, 2004). As a sophisticated geophysical phenomenon, earthquakes have dynamic processes that are irregular and nonlinear. This means that earthquake precursor parameters have high uncertainties. Therefore, to clarify the relation between an abnormality in the ionosphere and an earthquake, more case studies and analysis methods need to be explored.

* **Received** 21 June 2011; **accepted in revised form** 15 September 2011; **published** 10 December 2011.
♣ **Corresponding author. e-mail**: ydmgeomag@263.net

The DEMETER satellite has operated continuously for many years, accumulating abundant observation data to explore possible electron density anomalies both in space and time prior to earthquakes. To detect the possible precursors, the analysis method employed in this paper is based on a comparison of data recorded close to earthquakes in space and time and past data for the same area. Two famous earthquakes, the Pu'er and Wenchuan earthquakes, are analyzed in a case study. The electron density N_e recorded onboard the DEMETER satellite is briefly described in section 2. The analysis method is presented in section 3. Results are presented in section 4 and conclusions are given in section 5.

2 Data set

The dataset used is from the French DEMETER satellite. It is the first satellite, which is especially devoted to the investigation of the Earth ionosphere disturbances due to seismic and volcanic activities. Its scientific objectives are to study the ionospheric disturbances in relation to the seismic activity, volcano activity and anthropogenic activity, to contribute to the understanding of the generation mechanism of these disturbances, and to give global information on the Earth electromagnetic environment. The satellite was launched on June 29, 2004. It has a nearly circular Sun-synchronous orbit (10:30 LT in the day sector, 22:30 LT in the night sector). The orbital altitude was initially about 710 km and then adjusted to 660 km at the end of 2005, and the orbital inclination is 98°. The onboard scientific instruments make measurements between −65° and +65° in geomagnetic latitude (Cussac et al., 2006). The N_e data used in this paper were recorded by the ISL (Instrument Sonde de Langmuir) experiment onboard the satellite. The time resolution is 1 second. Details of ISL were given by Lebreton et al. (2006). Any potential changes due to seismic activity may be overwhelmed by the stronger influence of ionospheric ionization during the day (Nemec et al., 2008). Thus, this study only considers the nighttime data. Two well-known earthquakes, the Wenchuan and Pu'er earthquakes, with epicenters on the Chinese mainland, are chosen from the China Earthquake Networks Center catalog (http://www.csndmc.ac.cn/newweb/index.jsp) as case studies. The K_p index gives a good indication which describes how the Earth's magnetic field has been disturbed during the most recent three-hour period. It has been widely used in ionospheric and magnetospheric studies and is generally recognized as an index of worldwide geomagnetic activity. Therefore, to distinguish pre-earthquake anomalies from other anomalies related to geomagnetic activity, the K_p indexes given by the World Data Center in Kyoto (http://wdc.kugi.kyoto-u.ac.jp/index.html) are also taken into account.

3 Method

3.1 Spatial studies

In spatial searching for possible anomalies occurring before earthquakes, analysis is based on a comparison of data recorded spatially close to earthquakes and past data for the same area. In this section, robust two-step data processing has been applied. The first step is to divide the Earth's surface into cells with two-degree resolution both in latitude and longitude. A single earthquake can then be assigned to a cell according to its latitude and longitude, and a square area comprising 121 cells and centered around this earthquake cell is considered as the research area, as shown in Figure 1. The time resolution of the N_e data is 1 s, so about 30 s time interval and 30 data samples can contribute to one corresponding cell for one satellite orbit data.

					5					
					4					
					3					
					2					
					1					
5	4	3	2	1	EQ	1	2	3	4	5
					1					
					2					
					3					
					4					
					5					

Figure 1 Research area centered around one earthquake.

The second step in data processing is to extract anomalies at the time of each earthquake. It is known that the important work in extracting anomalies is to determine the normal background. Previous research has shown that variations in the ionosphere are extraordinarily complicated and highly dynamic (Sharma et al.,

2008). The background depends on solar and geomagnetic activities, season, latitude, longitude, altitude and other unknown parameters (Rishbeth, 1998; Zou et al., 2000; Chen et al., 2009). In addition, earthquakes occur at different times in different locations. It is impossible to give a unified background for all earthquakes. Therefore, a separate background was constructed for each earthquake by considering a shorter time span, the geomagnetic conditions and a smaller research region. This may be a better way to distinguish pre-earthquake anomalies from anomalies related to other parameters. In this section, all the data assigned to each research cells were collected during the given time interval. As the orbital repeat period of the DEMETER satellite is about 16 days, that is to say, an observation period of at least 16 days is necessary to ensure there are observation data for each cell. Considering the constraint on the K_p index (K_p<3+), an observation period of 30 days is better for accumulating cell data. When the background was expected to be quieter, a stricter constraint on the K_p index (K_p<2+) was applied, and a longer time span (31 to 75 days before the earthquake) is necessary to accumulate enough data. This time span and the K_p index constraint ensure that each cell has enough data as much as possible, so the effects of yearly and seasonal ionosphere variations and geomagnetic activities are avoided. To explore the pre-earthquake phenomena, only data for the period before the earthquake occurrence were used. For each cell, the data with K_p<2+ in the time interval of 31 to 75 days before the earthquake were used to construct the background, and the data with K_p<3+ in the time interval from 1 to 30 days before the earthquake were used for comparison. The orbit altitudes of the DEMETER satellite stabilized at around 660 km over four years, which reduced the effect of height on the data. Additionally, only nighttime data were used, which efficiently reduces the disturbance from solar activity.

The mean values of the background and analytical data are calculated and denoted by $\overline{b_{ij}}$ and $\overline{g_{ij}}$, respectively. They are expressed as

$$\overline{b_{ij}} = \frac{\sum_{t=-75}^{-31}\sum_{k=0}^{N_t} x_{ijtk}}{\sum_{t=-75}^{-31} N_t}, \tag{1}$$

$$\overline{g_{ij}} = \frac{\sum_{t=-30}^{-1}\sum_{k=0}^{N_t} x_{ijtk}}{\sum_{t=-30}^{-1} N_t}, \tag{2}$$

where the parameters x are the N_e values, N is the number of values in one day, i and j are the column number and row number of the cell respectively, t is the number of days before the earthquake (negative numbers refer to days before the earthquake), and k is the number of data in cell (i, j). According to Figure 1, i and j vary from −5 to +5. At the same time, the standard deviation of the background is calculated by

$$\sigma_{bij} = \sqrt{\frac{\sum_{t=-75}^{-30}\sum_{k=0}^{N_t}\left(x_{ijtk} - \overline{b_{ij}}\right)^2}{\sum_{t=-75}^{-31} N_t}}, \tag{3}$$

where σ_{bij} is the standard deviation of the background data collected for each cell. The variation in the data before each earthquake relative to the background data in each cell is then

$$R_{ij} = \frac{(\overline{g_{ij}} - \overline{b_{ij}})}{\sigma_{bij}}. \tag{4}$$

Finally, the relative variation for each cell is obtained from equation (4) and the anomaly distribution is presented.

3.2 Temporal studies

This section investigates the appearance time of possible anomalies. Analysis is based on the comparison of data recorded on one day and past data recorded over several days. The research area for each earthquake is the same as that in section 3.1, and the difference is that the entire research area is considered as one large cell (22-degree resolution both in latitude and longitude). The area is large enough for the satellite to pass over once a day. For the current day, the mean value of the data assigned to this large cell was calculated to represent the measurement value for the zone, denoted as $\overline{b'_t}$. The mean value and standard deviation of all data recorded in the time interval from 1 to 15 days before the current day in the same zone were calculated as the relative background and variation range, denoted respectively as $\overline{g'_t}$ and $\overline{\sigma'_t}$. These quantities are expressed as

$$\overline{b'_t} = \frac{\sum_{k=0}^{N_t} x_{tk}}{N_t}, \tag{5}$$

$$\overline{g'_t} = \frac{\sum_{t=-15}^{-1}\sum_{k=0}^{N_t} x_{tk}}{\sum_{t=-15}^{-1} N_t}, \tag{6}$$

and

$$\sigma'_{bt} = \sqrt{\frac{\sum_{t=-15}^{-1}\sum_{k=0}^{N_t}(x_{tk}-\overline{b_t})^2}{\sum_{t=-15}^{-1}N_t}}. \quad (7)$$

The data series for a long period around an earthquake occurrence is then analyzed to determine a possible anomaly.

4 Results

The data processing method introduced above was applied to the analysis of two earthquakes. Detailed information of the earthquakes is listed in Table 1. The analysis results for the two earthquakes are presented as follows.

Table 1 Investigated earthquakes

No.	Origin time (UTC)		Lat./°N	Long./°E	Depth/km	M_S	Location
	a-mo-d	h:min:s					
1	2007-06-02	21:34:56	23.0	101.1	33	6.4	Pu'er, Yunnan
2	2008-05-12	06:28:04	31.0	103.4	14	8.0	Wenchuan, Sichuan

The first earthquake is the Pu'er earthquake with a magnitude M_S6.4. The earthquake occurred at 21:34 (UTC) on June 2, 2007 and located in Yunnan province (23.0°N, 101.1°E). The analysis result is presented in Figure 2. Figure 2a is obtained for the spatial domain from equation (4). It shows the comparison between the data immediately before the event time and earlier data for the same cells. The center of the rectangular zone is the position of the epicenter. As shown in Figure 2a, there are two significant increases in density close to the epicenter, one to the north of the epicenter and the other to the south-east. Additionally, there is an obvious decrease in density at a relatively distant location to the south-west. There are no other anomalies in the research region. Figure 2b is a time series of the variation in electric density. The black dots indicate the average value calculated from the data collected for the rectangular zone in one day, and they are joined with a black line. A point where the line is broken indicates that data are missing for that day. The red line shows the background obtained from equation (6), and the broken red line indicates the one-standard-deviation range. The color bars indicate earthquakes with magnitude. The green line shows the position of the current earthquake. As displayed in Figure 2b, the days before this event were not quiet and there was disturbance from other three earthquakes as listed in Table 2. There are disturbances beyond the one-standard-deviation range before each earthquake.

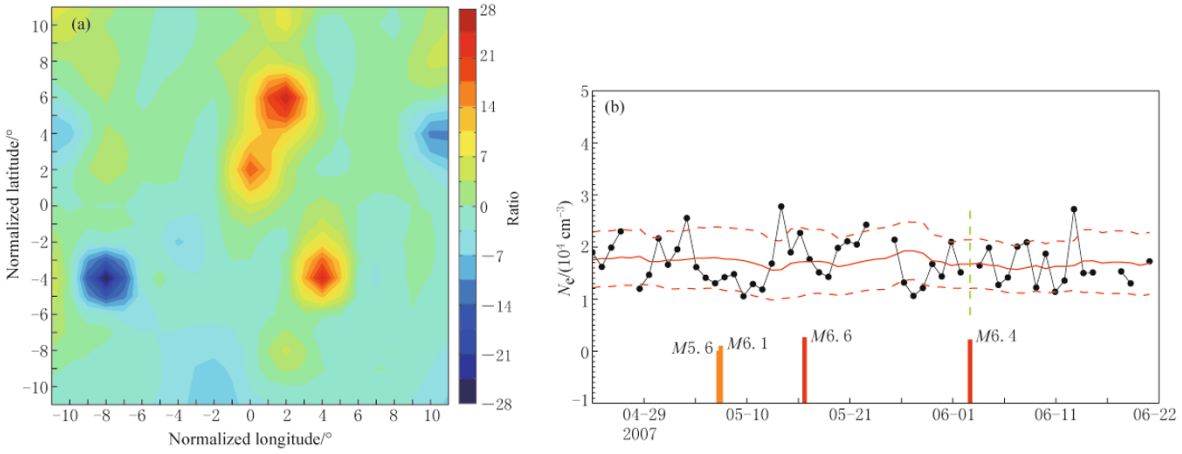

Figure 2 Analysis result for the Pu'er earthquake. (a) Anomaly distribution. (b) Time series of N_e during the earthquake.

Table 2 The earthquakes occurred before Pu'er earthquake

No.	Origin time (UTC)		Lat./°N	Long./°E	Depth/km	M_S	Location
	a-mo-d	h:min:s					
1	2007-05-05	08:51:41	34.3	81.9	33	6.1	Tibet
2	2007-05-07	11:59:49	31.5	97.8	33	5.6	Tibet
3	2007-05-16	08:56:16	20.6	101.0	33	6.6	Laos

As previous works on precursors have shown anomalies appeared prior to earthquake occurrence and located near the epicenter (Zaslavski et al., 1998; Liu et al., 2004; Kon et al., 2010). Meanwhile, previous studies on the Pu'er earthquake using a different method found that the spatial images of N_e exhibited high values near the epicenter for 30 days before the earthquake and there was good correlation between an anomaly and distribution of earthquakes in space and time (Ouyang et al., 2008; Zhu et al., 2008). This result in this study shows good consistency with the conclusions of those studies.

Similarly, the two analysis methods mentioned above are applied to the second event, the Wenchuan M_S8.0 earthquake. This earthquake occurred at 06:28 (UTC) on May 12, 2008 in Sichuan province (31.4°N, 104.1°E). Similar increases and decreases in density are seen close to the epicenter, as presented in Figure 3a. Additionally, there was a disturbance beyond one-standard-deviation before the Wenchuan earthquake (Figure 3b).

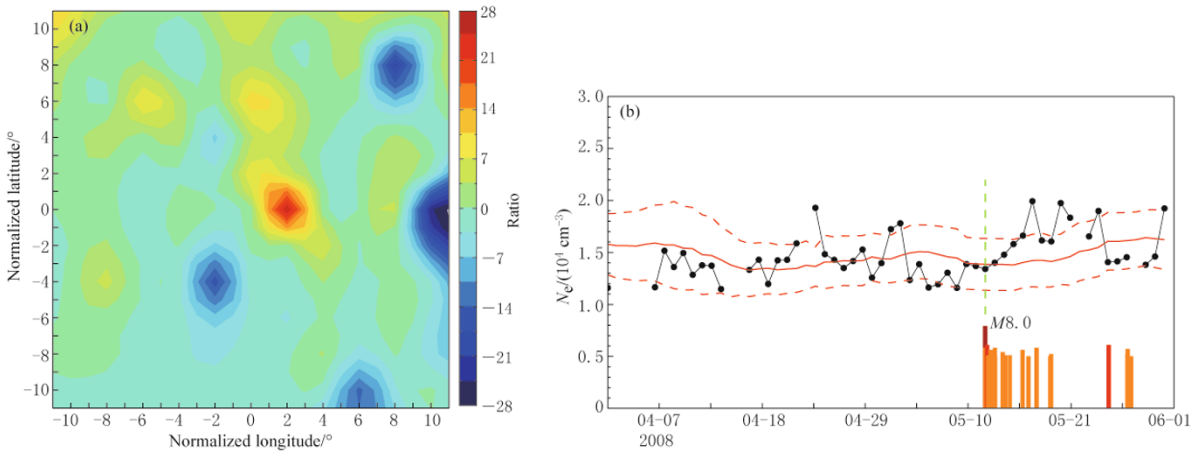

Figure 3 Analysis result for the Wenchuan earthquake. (a) Anomaly distribution; (b) Time series of N_e during the earthquake.

Abnormalities before the Wenchuan earthquake were also reported in previous papers. Zhang et al. (2009) reported a position where the ion temperature increased before the Wenchuan earthquake. This shows good consistency with the position where the N_e has an increasing anomaly in this paper. They also calculated the daily averaged values of N_i (ion density) during the local nighttime from May 1 to 12 on the scale of 20°N–40°N and on up-orbits within 2 000 km of the epicenter, and found the lowest value three days before the Wenchuan earthquake. The variation trend is the same as that of the N_e in time series. Zeng et al. (2009) indicated that N_e decreased three days before the Wenchuan earthquake, and the oxygen ion density increased seven days before the earthquake. As the tracks of DEMETER orbits passing through the southwest research region three days before the earthquake and through the northeast seven days before the earthquake, and the balance existing between N_e and N_i, the results agree well with the results of the present study. In addition, there are no other earthquakes before the Wenchuan earthquake. All evidence demonstrates a close relationship between the disturbances and the earthquake preparation.

5 Discussion

The spatial studies of the two events showed that there were positive anomalies near their epicenters prior to the earthquake occurrences, sometimes accompanied by a negative anomaly. The position of an anomaly is uncertain, as the anomaly is sometimes to the north of the epicenters and sometimes to the south. The difference in position may be due to the different earthquake types; in any event, the anomaly is close to the epicenter. Anomalies are located close to the preparation zone estimated by Dobrovolsky et al. (1979).

The time-series studies indicate that there are disturbances prior to earthquake occurrence. However, there were other earthquakes during the analysis period for the Pu'er earthquake in the research area. Therefore, the post-seismic effects may be considered as pre-seismic effects. It is thus difficult to distinguish the source of the anomalies. However, this problem of aftershocks is only minor because we understand the physical phenomena that occur at the time of earthquakes, e.g., the propagation of an acoustic-gravity wave (which can perturb the ionosphere), the effect of which lasts only a few hours.

Both the spatial and temporal results show good consistency with those of previous works. This suggests that these anomalies have a close relation with earthquake preparation. As an earthquake is a sophisticated geophysical phenomenon, it has many factors such as magnitude, depth, location and mechanism. Therefore, to determine whether anomalies are a common feature of most earthquakes, more case studies and statistical works are needed. With further research, the relation between these anomalies and earthquakes will be clarified.

Acknowledgements The authors are grateful to the Guest Investigator programme issued by CNES for the DEMETER mission for supplying the raw data and thank the reviewers for their constructive comments. This study was supported by the National Key Technology Research and Development Programme of China (No. 2008BAC35B02).

References

Akhoondzadeh M, Parrot M and Saradjian M R (2010). Electron and ion density variations before strong earthquakes (M>6.0) using DEMETER and GPS data. *Nat Hazards Earth Syst Sci* **10**: 7–18.

Chen Y, Liu L, Wan W, Yue X and Su S Y (2009). Solar activity dependence of the topside ionosphere at low latitudes. *J Geophys Res* **114**: A08306, doi:10.1029/2008JA013957.

Chmyrev V M, Isaev N V, Bilichenko S V and Stanev G (1989). Observation by space-borne detectors of electric fields and hydromagnetic waves in the ionosphere over an earthquake center. *Phys Earth Planet Int* **57**: 110–114.

Cussac T, Clair M A, Ultre-Guerard P, Buisson F, Lassalle-Balier G, Ledu M, Elisabelar C, Passot X and Rey N (2006). The DEMETER microsatellite and ground segment. *Planet Space Sci* **54**: 413–427.

Dobrovolsky I P, Zubkov S I and Miachkin V I (1979). Estimation of the size of earthquake preparation zones. *Pure Appl Geophys* **117**: 1 025–1 044, doi:10.1007/BF00876083.

Gokhberg B M, Pilipenko A V and Pokhotelov A O (1983). Seismic precursors in the ionosphere. *Izvestiya Earth Physics* **19**: 762–765.

Hayakawa M (1999). *Atmospheric and Ionospheric Electromagnetic Phenomena Associated with Earthquakes*. Terra Sci. Pub. Co., Tokyo, 997pp.

Hayakawa M and Molchanov O A (2002). *Seismo-Electromagnetics*: *Lithosphere-Atmosphere-Ionosphere Coupling*. Terra Sci. Pub. Co., Tokyo, 477pp.

He Y, Yang D, Chen H, Qian J, Zhu R and Parrot M (2009). SNR changes of VLF radio signals detected onboard the DEMETER satellite and their possible relationship to the Wenchuan earthquake. *Science in China* (*Series D*) **52**: 754–763, doi:10.1007/s11430-009-0064-5.

Kon S, Nishihashi M and Hattori K (2010). Ionospheric anomalies possibly associated with $M\geq$6.0 earthquakes in the Japan area during 1998–2010: Case studies and statistical study. *J Asian Earth Sci* **41**: 410–420, doi:10.1016/j.jseaes.2010.10.005.

Larkina V I, Nalivaiko A V, Gershenzon N I, Gokhberg M B, Liperovsky V A and Shalimov S L (1983). Observations of VLF radiations linked with seismic activity from Intercosmos-19 satellite. *Geomagn Aeron* **23**: 842–847.

Lebreton J P, Stverak S, Travnicek P, Maksimovic M, Klinge D, Merikallio S, Lagoutte D, Poirier B, Blelly P L, Kozacek Z and Salaquarda (2006). The ISL Langmuir probe experiment processing onboard DEMETER: Scientific objectives, description and first results. *Planet Space Sci* **54**: 472–486.

Liu J Y, Chuo Y J, Shan S J, Tsai Y B, Chen Y I, Pulinets S A and Yu S B (2004). Pre-earthquake ionospheric anomalies registered by continuous GPS TEC measurements. *Ann Geophys* **22**: 1 585–1 593.

Molchanov O A (1993). Wave and plasma phenomena inside the ionosphere and magnetosphere associated with earthquakes. In: Stone W R ed. *The Review of Radio Science* (1990–1992). Oxford Univ. Press, London, 591–600.

Nemec F, Santolik O, Parrot M and Berthelier J J (2008). Spacecraft observations of electromagnetic perturbations connected with seismic activity. *Geophys Res Lett* **35**: L05109, doi:10.1029/2007GL032517.

Ouyang X Y, Zhang X M, Shen X H, Liu J, Qian J D, Cai J A and Zhao S F (2008). Ionospheric N_e disturbances before 2007 Pu'er, Yunnan, China, earthquake. *Acta Seismologica Sinica* **21**: 425–437, doi:10.1007/s11589-008-0425-8.

Parrot M and Johnston M (1993). Special Issue: Seismoelectromagnetic Effects. *Phys Earth Planet Int* **77**: 1–137.

Parrot M and Mogilevsky M M (1989). VLF emissions associated with earthquakes and observed in the ionosphere and the magnetosphere. *Phys Earth Planet Int* **57**: 86–99.

Parrot M, Berthelier J J, Lebreton J P, Sauvaud J A, Santolik O and Blecki J (2006). Examples of unusual ionospheric observations made by the DEMETER satellite over seismic regions. *Phys Chem Earth* **31**: 486–495, doi:10.1016/j.pce.2006.02.011.

Pulinets S A and Boyarchuk K A (2004). *Ionospheric Precursors of Earthquakes*. Springer Verlag Publ., Berlin, 129–169.

Pulinets S A and Legenka A D (2003). Spatial-temporal characteristics of the large scale disturbances of electron concentration observed in the F-region of the ionosphere before strong earthquakes. *Cosm Res* **41**: 221–229.

Rishbeth H (1998). How the thermospheric circulation affects the ionospheric F2-layer. *J Atmos Terr Phys* **60**(14): 1 385–1 402.

Rozhnoi A, Solovieva M, Molchanov O, Akentieva O, Berthelier J J, Parrot M, Biagi P F and Hayakawa M (2008). Statistical correlation of spectral broadening in VLF transmitter signal and low-frequency ionospheric turbulence from observation on DEMETER satellite. *Nat Hazards Earth Syst Sci* **8**: 1 105–1 111, doi:10.5194/nhess-8-1105-2008.

Rozhnoi A, Solovieva M, Molchanov O, Biagi P F, Hayakawa M, Schwingenschuh K, Boudjada M and Parrot M (2010). Variations of VLF/LF signals observed on the ground and satellite during a seismic activity in Japan region in May–June 2008. *Nat Hazards Earth Syst Sci* **10**: 529–534.

Sarkar S, Gwal A K and Parrot M (2007). Ionospheric variations observed by the DEMETER satellite in the mid-latitude region during strong earthquakes. *J Atmos Sol Terr Phys* **69**: 1 524–1 540.

Sharma K, Das R M, Dabas R S, Pillai K G M, Garg S C and Mishra A K (2008). Ionospheric precursors observed at low latitudes around the time of Koyna earthquake. *Adv Space Res* **42**: 1 238–1 245.

Zaslavski Y, Parrot M and Blanc E (1998). Analysis of TEC measurements above active seismic regions. *Phys Earth Plan Int* **105**: 219–228.

Zeng Z C, Zhang B, Fang G Y, Wang D F and Yin H J (2009). The analysis of ionospheric variations before Wenchuan earthquake with DEMETER data. *Chinese J Geophys* **52**(1): 11–19 (in Chinese with English abstract).

Zhang X, Shen X, Liu J, Ouyang X, Qian J and Zhao S (2009). Analysis of ionospheric plasma perturbations before Wenchuan earthquake. *Nat Hazards Earth Syst Sci* **9**: 1 259–1 266.

Zhu R, Yang D M, Jing F, Yang J Y and Ouyang X Y (2008). Ionospheric perturbations before Pu'er earthquake observed on DEMETER. *Acta Seismologica Sinica* **21**: 77–81, doi:10.1007/s11589-008-0077-8.

Zou L, Rishbeth H, Muller-Wodrag I C F, Aylward A D, Millward G H, Fuller-Rowell T J, Idenden D W and Moffett R J (2000). Annual and semiannual variations in the ionospheric F2-layer. I. Modelling. *Ann Geophys* **18**: 927–944.